International Journal of Science and Research Archive

eISSN: 2582-8185

Cross Ref DOI: 10.30574/ijsra

Journal homepage: https://ijsra.net/

(RESEARCH ARTICLE)

Check for updates

Development of three-dimensional seismograph for evaluation of seismic effects of earth disturbances

Adewumi Thompson Obagade *, Sunday Emmanuel Falodun and Theophilus Ewetumo

Department of Physics, Federal University of Technology, P.M.B. 704, Akure, Nigeria.

International Journal of Science and Research Archive, 2024, 12(01), 2316–2333

Publication history: Received on 23 April 2024; revised on 31 May 2024; accepted on 03 June 2024

Article DOI: https://doi.org/10.30574/ijsra.2024.12.1.1002

Abstract

This research presents the development of a triaxial seismograph; a device used to measure ground vibration levels in three perpendicular directions. The device comprises three triaxial geophone networks that can be positioned at three different points on the ground surface to measure ground vibration levels, five 24-bit analogue-to-digital converters (ADCs) to digitize the geophones' analogue outputs, an Arduino-Mega microcontroller that coordinates the operations of the system's components, five multiplexers (MUXs) which serves as an interface switch between the ADCs and the microcontroller, a Liquid Crystal Display (LCD), and a MicroSD card for data storage. Comparative analysis of the data measured by the seismograph with that of a standard seismograph showed a very good relation and this demonstrates the reliability of the developed device. After calibration, the seismograph can measure ground vibration levels in terms of peak particle velocity (PPV) ranging from 0.000017 mm/s to 143 mm/s with a sensitivity of 0.00000424 mm/s. Fast Fourier Transform (FFT) analysis of the result of vibration tests carried out at various field locations indicates that the seismograph performed satisfactorily according to the design specifications. Also, from the analysis, it was seen that the vibration amplitudes obtained at each site locations are slightly above the threshold limit. Cost analysis reveals the affordability of the seismograph compared to standard models, making it a viable option for laboratories, research, and demonstrations. The cost-effectiveness and accuracy of the device enhances its utility, positioning it as a potential replacement for more expensive options in the market.

Keywords: Seismograph; Geophone; Arduino-Mega Microcontroller; Multiplexer; Ground vibration level

1. Introduction

Over the last few years, every regions of the world have continued to witness steady increase in the development of infrastructures and exploration of mineral resources. The earth's surface has become more susceptible to disturbances due to these activities. On this note, people experience has confirmed rising cases of vibrations as one of the most noticeable and immediate effects of earth disturbances. These worrisome occurrences continue to eat deep into our environment; thereby leading to several environmental problems within the society, most especially in densely-populated urban areas or cities around the world. [1,2] described earth disturbances as phenomena or any event that disrupts the natural balance of the particles of the earth crust. Consequently, leads to the release of some form of energy stored within the earth as the mass particles of the earth strained against one another. The energy released during these interactions often propagates through the earth and its surface in form of seismic waves [3], and as these waves pass through a given point on the earth, it creates a wide range of effects such as ground shakings generally known as ground vibrations.

According to [4, 5-7] earth disturbances can be caused by different factors, including natural activities such as earthquake, volcanic eruption, tsunami, landslide, microseism, molten magma movement, thunderstorm, windstorm, rainstorm, ocean waves, among others. Aside from these natural factors, man-made or artificial activities such as mining

* Corresponding author: Obagade T. A

and quarry blasting operation, drilling, excavation, demolition, explosion, piling, weight dropping, hammering, movement of a large number of people footsteps, road and railway traffic, road construction work, sonic booms, machineries in nearby locations, among others are also known as major causative factors that trigger earth disturbances [4, 5, 8-12].

[13] revealed that if the magnitude of the energy released is large enough to generate high vibration intensity, ground may vibrate to a level that it can cause severe discomfort or failure in surrounding structures and in many cases, the ground surface may get ruptured; thereby leading to devastations of the geological features of the environment. Prolonged exposure of environment to ground vibrations, especially of those that exceed the safe limits or with sufficiently high levels may create damage to nearby buildings and other structures which may lead to some cosmetic or minor effects such as rattling of window panes, crumbling and falling of wall plasters, shaking of items on shelves or hanging on walls, cracking of building walls and rupturing of underground utilities such as buried pipelines [1, 7, 14-16].

As a matter of fact, long-term effect of these minor damages in critical cases could result in total collapse, especially in structures in a weak condition or those that have lost integrity to carry their original design loads [17]. Apart from the potential damages on structures; however, ground vibrations may create rumble sounds or noises which may cause annoyance to the occupants of the nearby buildings closer to the area of occurrence, thereby leading to serious complaints [14, 16, 18, 19] and owing to this, concern has also arisen over this effect.

[4, 8, 9, 20-22] revealed that man-made or artificially generated ground vibrations have become more of interest to scientists and engineers in recent time as this is evident in our everyday life and make up most of the seismic or earth disturbances generated in our environment even in regions with little or no natural seismic conditions. Consequently, to properly predict how much vibration levels that are transmitted through the ground from the source, and the dynamic response of structures to vibratory forces from this event, there has been a considerable interest in the vibration control study as an active research field in the last decades from both seismological and engineering point of view in an attempt to mitigate and also restrict the effects of vibrations from expanding to buildings and other structures [23]. Therefore, to enhance evaluation of ground vibration levels and structural response to this effect, it has become necessary to monitor ground vibrations by the use of field test techniques using seismograph rather than the theoretical, numerical and simulation methods that have been used in previous times, as these methods are insufficient enough to accurately assess the true levels of ground vibrations that occur in a given area [14, 24].

In respect to this, several studies have shown the importance of seismographs in monitoring and predicting ground vibration effects. [25] developed a low-cost strong motion seismograph using a Micro-electromechanical (MEMS) silicon accelerometer to monitor strong motion signals. [26] employed a wireless seismic array system for monitoring seismic signals and noise generated during geological events. [27] developed single 3D geophones with alarm system to record the ground motion velocity induced by debris flows during quarry blasting operation. [22] used a triaxial vibration sensor to record and analyze the characteristics of seismic waves generated from blasting operations and their responses on structures. [28] developed a seismograph with accelerometer transducer to carry out awareness program on effects of seismic events. [29] designed a wireless geophone network with enhanced signal processing capability for effective detection of landslides. [30] used an Arduino based seismograph with accelerometer sensors to raise awareness of earthquake hazard and mitigation to group of high school students in Italy. [31] developed a low-cost single axis Arduino based seismic recorder using geophone sensors to record seismic signals from vertical component vibration.

In this work, focus was laid on developing a seismograph with three distinct triaxial geophone networks that is capable of monitoring and recording ground vibration levels resulting from seismic effects of earth disturbances due to human activities at different points along the ground surface.

2. Materials and methods

2.1. The Design Architecture of the Developed Seismograph

The architecture of the seismograph is illustrated in the block diagram shown in Figure 1. The block diagram presents how the hardware components are integrated with one another and the flow of data from the sensors to storage. Basically, the seismograph consists of six main units: sensing unit, signal conditioning unit, interface switch unit, signal processing unit, display unit and storage unit. Detailed discussions of the design of circuits in each unit are presented in the subsequent sections.

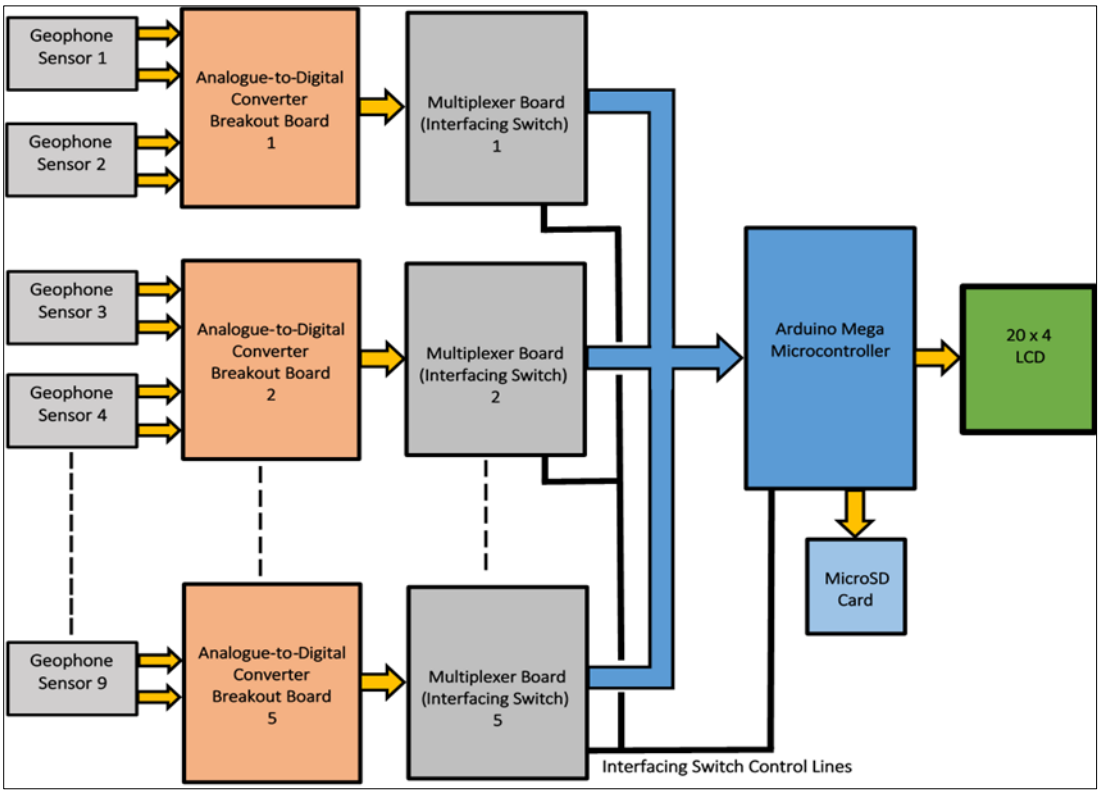

Figure 1 Block Diagram of the developed Seismograph

2.2. Hardware Overview

2.2.1. Sensor

The sensor chosen for this work is SM-24 model geophone sensor manufactured by I/O sensor Netherland. The sensor is an electromagnetic transducer that generates electrical voltage signal corresponding to the velocity of ground motion detected. The sensor has a sensitivity of 28.8 V/m/s and a natural frequency of 10 Hz that spans up to 250 Hz. The sensor has several advantages such as its ability to work without any power source and as well as its stability under temperature variation. All these make it a suitable choice of sensor for this work when compared to other vibration sensors. In this work, nine of this geophone sensor was used to carry out the study. The sensors were arranged such that they constitute three distinct sensing points along the ground surface. The sensors were implanted in a cubic wooden box having a dimension of 10 cm x 10 cm x 10 cm and were arranged in a three mutually perpendicular manners: two horizontal (*x*- and *y*-axes) and one vertical (*z*-axis) as depicted in Figure 2.

To ensure accurate measurements when one signal has been detected as well as preventing the sensors from prolonged oscillation after the ground has ceased to vibrate, the sensors were electrically damped by shunting their coil terminals with moderate resistors of 1 kilo-ohm (kΩ) to prepare the sensors readiness to receive the arrival of next seismic signals. When the coils move, the induced voltages due to the motions of the coils in the magnetic fields of the permanent magnets within the sensors causes currents to flow through the resistors.

According to Lenz's Law, these currents oppose the motions of the coils and thus, cause damping. So, when vibration occurs and the ground shakes, the sensors' house casings moves with it, thereby causes a relative motion between the coils and the magnet mass within the sensors, which results in the generation of electrical voltage signals that is proportional to the velocity of ground motions detected. The generated signals by the geophones are relatively very small, typically in the range of few microvolts (μV) to millivolts (mV). Consequently, the signals may be vulnerable and susceptible to noise and other parasitic interference; hence, they are needed to be conditioned, typically they are to be filtered and amplified before being passed to the other circuits for further processes such as recording.

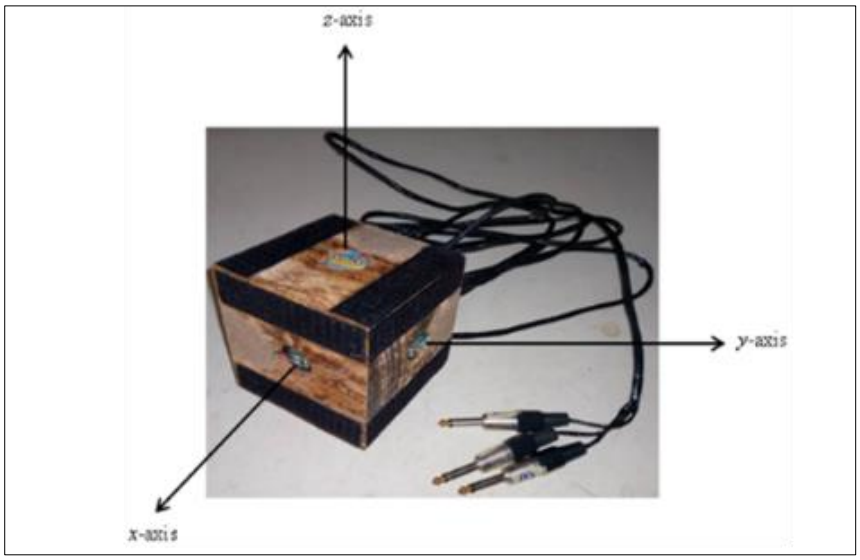

Figure 2 Three Dimensional Arrangement of the Geophone Sensors

2.2.2. Signal Conditioners

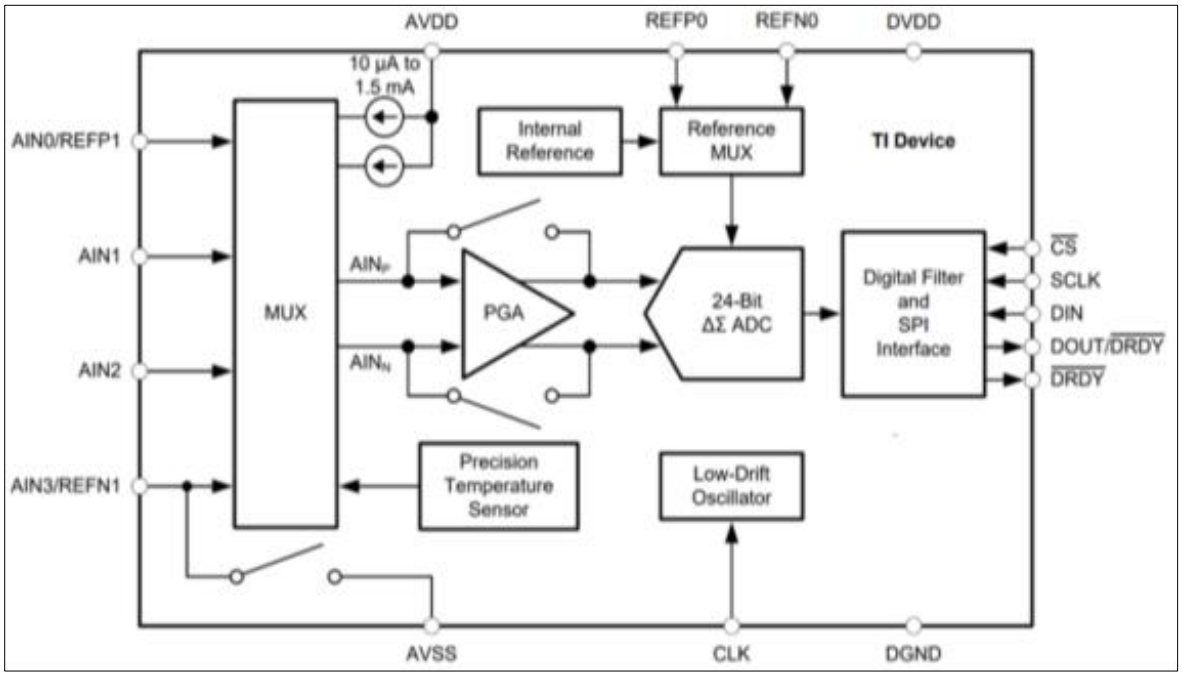

Figure 3 The Internal Structure of ADS1220 Analogue-to-Digital Converter Breakout Board

The output signals from the geophones are very small, typically in the range of few microvolts (µV) to millivolts (mV). Consequently, they may be vulnerable with noise; thus, they are required to be conditioned before being transformed into digital formats for further processes. This includes filtering to remove noise from the geophones' signals and amplification to increase the geophones' signal amplitudes to the levels that they can be correctly detected by the Analogue-to-Digital Converters (ADCs). However, to measure the motion of ground surface as a result of propagation of seismic waves through the ground requires greater precision, so the low resolution Analogue-to-Digital Converters (ADCs) like one in Arduino microcontrollers are unable to provide the required resolution needed for this work. Hence, an external ADCs such as that of high resolution 24-bit sigma delta ADS1220 ADC breakout board from Olimex Instrument with wide supply range of 2.3 V to 5.5 V, programmable gains up to 128 V/V and a programmable data rates up to 2000 samples per second (SPS) was employed to implement the design. Figure 3 shows the internal structure of the ADC breakout board. According to the diagram, the board is integrated with number of built-in components such as input multiplexer (MUX), analogue input filter, low noise programmable gain amplifier (PGA), modulator,

programmable digital decimating filter, an internal voltage reference (V_{ref}), internal oscillator, and others. All the aforementioned features made the board a choice of component that is adequate for this work as it reduces the complexity, bulkiness, system cost, and eliminate the requirement for the use of external circuits. The ADC boards operation were based on software instructions from microcontroller.

2.2.3. Input Multiplexers

The input multiplexers of the ADCs are four input channel multiplexers that allow input sensors to be connected to the Analogue-to-Digital Converters either in four single-ended inputs or two differential inputs. In this work, the multiplexers were programmed in such a way that geophones' output signals are connected to the ADCs in two differential input as shown in Figure 4.

2.2.4. Filters and Amplifiers

As previously mentioned, the signals produced by the geophone sensors are relatively very small; typically, in the range of few microvolts (μV) to millivolts (mV) which may make the signals to be susceptible to noise or interference. Hence, it is necessary to remove this noise from the signals before being passed to other circuits for further processes. The ADCs uses oversampling technique to sample the applied input signals. The high sampling rate allows the adoption of antialiasing filter process and thus, help to avoid a type of distortion called aliasing.

The analogue input filters located prior to the amplifiers unit of the device are electromagnetic filters; the filters were used to eliminate any high frequency noise that might present in the geophones' output signals due to effects of electromagnetic interference which may corrupt the ADCs' inputs. The amplifiers are basically low noise programmable gain amplifiers (PGAs). The amplifiers were programmed with a gain factor of 4 to amplify the geophones' outputs to the levels that can be detected by the ADCs' modulators, wherein the analogue-to-digital conversion processes take place. Once the geophone signals are filtered and amplified, they are passed to the ADCs' modulators for digital processing.

2.2.5. Analogue-to-Digital Converters (ADCs)

The modulators are the main component of the ADC boards wherein the analogue-to-digital conversion processes take place. The ADCs were drive with a frequency signal of 4.096 MHz provided by the on chip board internal oscillators and the internal clocks were used for one major reason; as it does not require any use of external components.

The ADCs were programmed such that the modulators samples the geophones' output signals at a frequency rate of 256 kHz to produce pulse code modulated (PCM) data streams which are transmitted as 24-bit serial digital signals. In addition, the ADCs were programmed in its normal mode operation, making it possible for the decimators to select the desired output data rate ranges from 20 SPS to 1000 SPS. After the analogue-to-digital conversion processes, the digital generated signals are passed to the digital decimating filters which comprises, digital filters and decimators.

2.2.6. Digital Filters and Decimators

The digital filters are basically Finite Impulse Response (FIR) filters which employed a low-pass filtering function to strips off any quantization error or noise components that might present in the serial digital output signals from the modulators during quantization process. The digitally filtered signals are passed to the decimators where the sampling rates are efficiently reduced to the desired output data rate. The ADCs were programmed in its normal mode operation, making it possible for the ADC boards to select the desired output data rate ranging from 20 SPS to 1000 SPS. In this study, the ADCs were programmed with a desired output data rate of 1000 SPS to decimate the digitally oversampled outputs from the modulators. This data rate was chosen so that the ADCs can accurately record the entire measurement bandwidth within the frequency range of 10 Hz to 250 Hz the geophones' signals. After the digital conversion processes, the digitally generated signals are passed to the microcontroller for further processing.

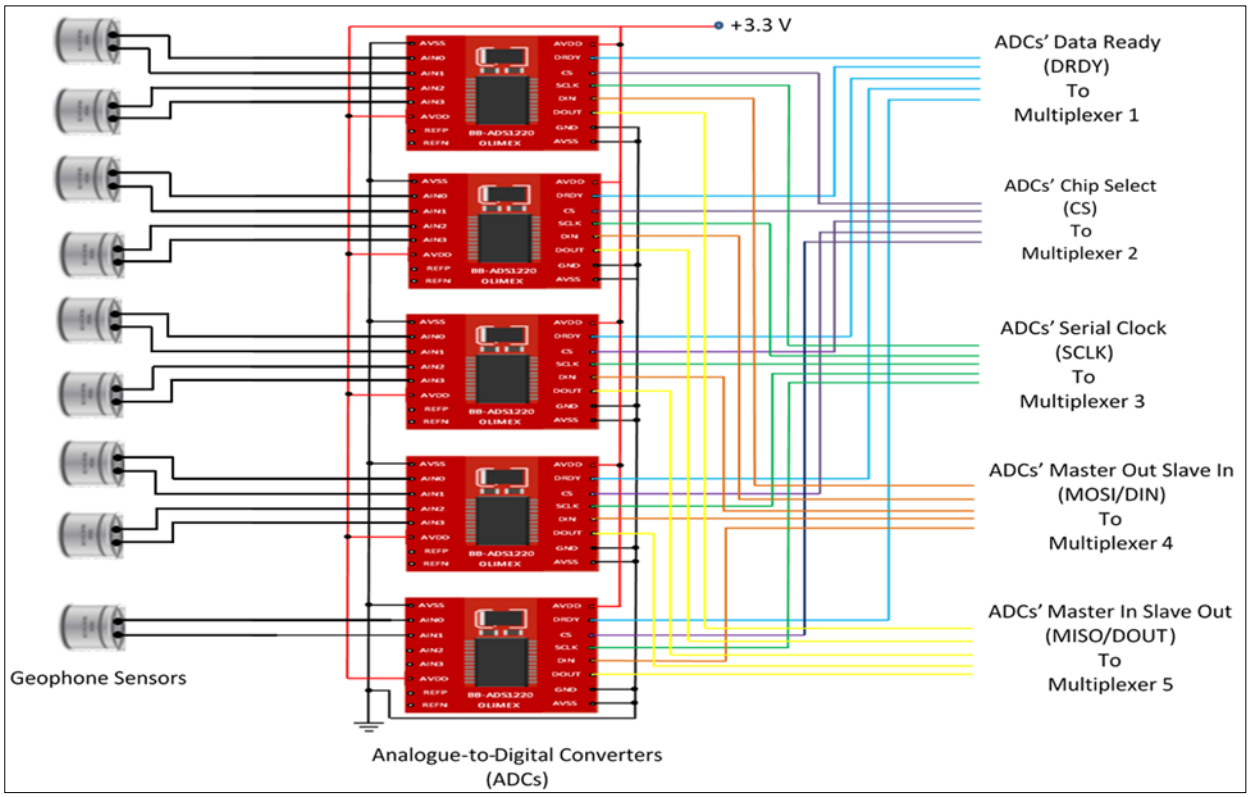

Figure 4 Schematic Diagram of the Geophone Sensors Connections with Analogue-to-Digital Converters (ADCs)

2.2.7. Analogue-to-Digital Converters (ADCs) connection with Microntroller

The ADCs shared the same single SPI bus with one another to communicate with the microcontroller. Therefore, to make the communication possible as well as preventing the ADCs' output signals from interfering with one another when communicating with the microcontroller; a digitally controlled analogue switch was employed to selectively take in turn the connection of the ADCs simultaneously with the microcontroller. The switch formed the interface between the ADCs and the microcontroller. The switch was accomplished using 74HC4051, a single-pole octal-throw (SP8T) multiplexer/demultiplexer breakout board. The multiplexer board has eight independent input/output pins, numbering (Y0, Y1, Y2, Y3, Y4, Y5, Y6, and Y7), a common input/output (Z), three digital control inputs (S0, S1 and S2), and enable input (E). The multiplexers were configured using Synchronous Time Division Multiplexing (STDM) technique, a technique in which multiple input signals are allowed to be transmitted simultaneously over a single line using the same time slots. Five of this multiplexer board was used to selectively take in the ADCs simultaneously to communicate with the microcontroller. As illustrated in the schematic circuit diagram of the switch shown in Figure 5, only five input pins Y0 to Y4 of the multiplexers were used to take in the ADCs output signals with the microcontroller. The ADCs selection was based on the combinations of HIGH and LOW logic levels placed on the control inputs (S0, S1 and S2) of the multiplexers by the microcontroller. The pins were connected to the digital pins 14, 15 and 16 of the microcontroller respectively. Figure 6 shows hardware implementation of the digital controlled analogue interfacing switch.

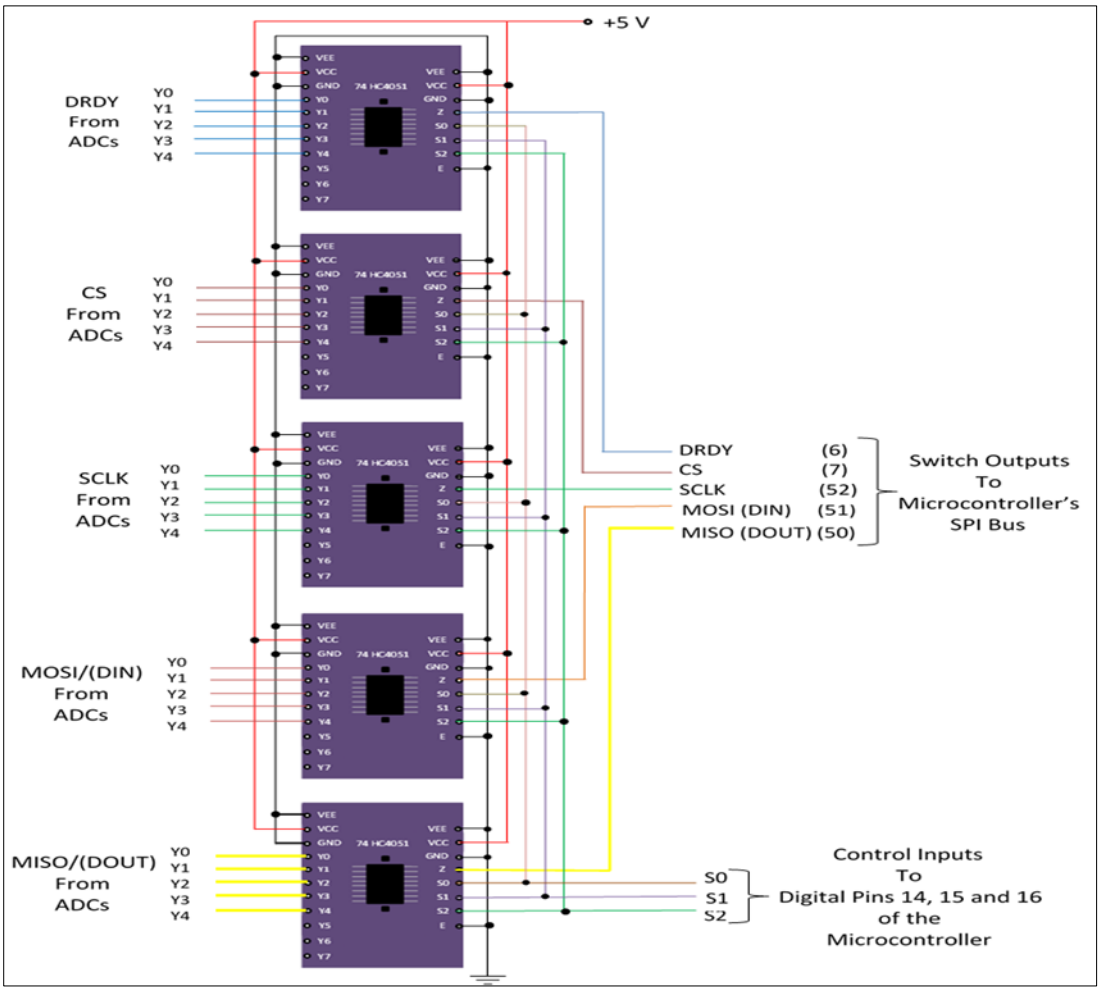

Figure 5 Schematic Circuit Diagram of the Digital Controlled Analogue Interfacing Switch

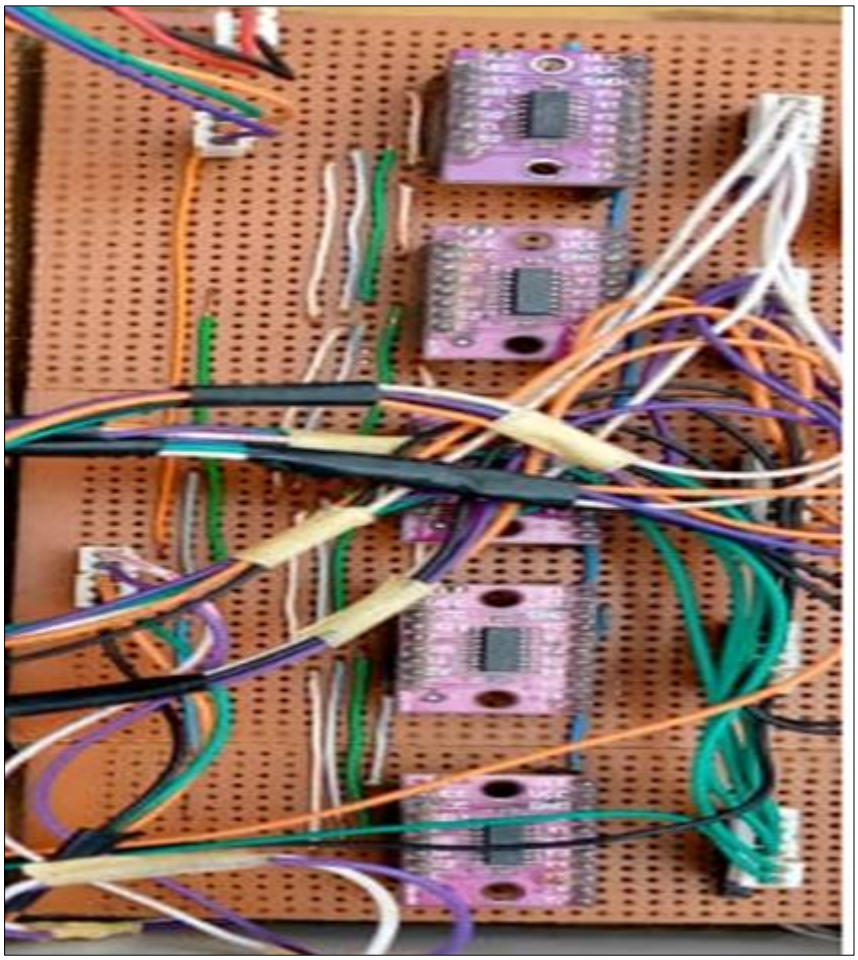

Figure 6 Hardware Connection of Multiplexers for the Realization of Digital Controlled Analogue Interfacing Switch

2.3. Microcontroller

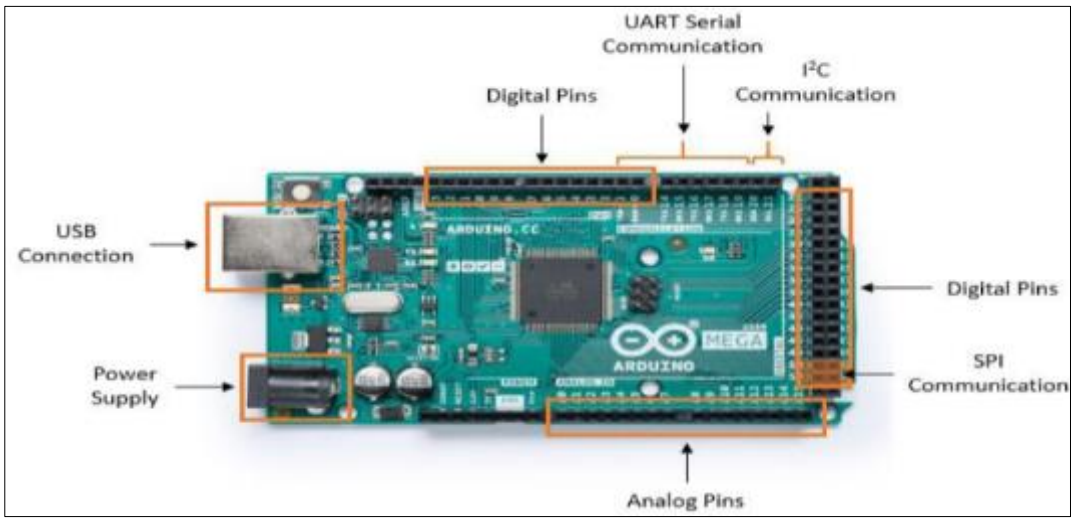

Figure 7 Arduino Mega2560 Microcontroller Board

The Arduino Mega2560 microcontroller was the choice of microcontroller used to capture data from the sensors through the ADCs. As stated previously, the ADCs communicate with the microcontroller over the SPI communication protocol. The microcontroller is set up as a master device which uses dedicated active low chip select (CS) and data ready (DRDY) pins along with the standard SPI pins for communication with the ADCs set up as slave devices. The

microcontroller being the heart of the device that controls all the operations of the components of the system was programmed in an integrated development environment (IDE) using C++ programming language to process the sensors' output signals through the ADCs into readable values that correspond to the levels of ground motions detected. Figure 7 shows the Arduino Mega2560 microcontroller with some of its features highlighted.

2.4. Liquid Crystal Display (LCD)

The display screen used in this project to display the values of vibration levels measured by the seismograph is 20 x 4 LCD module. The LCD is a type of display that measures 20 characters wide and 4 lines high. There are 16 pins in whole of the LCD and it can be connected to microcontrollers in two different modes; 8-bit and 4-bit modes.

In this work, the LCD is connected to the microcontroller using 4-bit connection mode and in this case, only 6 of the LCD's pins which include EN, RS, D4, D5, D6 and D7 are used to connect the LCD with the microcontroller as shown in Figure 8. So, the LCD's register pins D4 to D7 were connected to the microcontroller's digital pins 4 to 7. The enable (EN) pin is connected to the digital pin 8 and the register select (RS) pin is connected to the digital pin 9 respectively. However, the variable resistor 10 kΩ in the circuit control the contrast or brightness of the LCD. The LCD is known for its low power consumption and it can be powered with a maximum voltage of +7 V. But, in this work, the LCD was powered with a voltage of +5 V provided by the generic power output on the microcontroller.

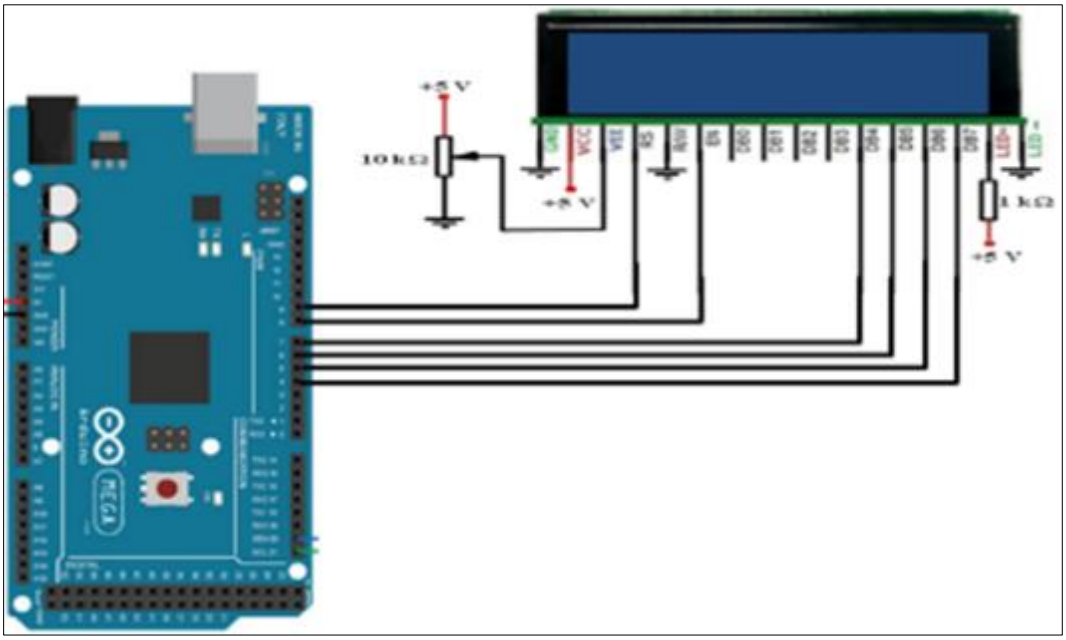

Figure 8 Hardware Connection of the Liquid Crystal Display with Microcontroller

2.5. MicroSD Card Modules

The microSD card modules used to store the ground motion levels measured by the seismograph are combinations of a Secure Data (SD) card shield adapter/reader, developed by Seed Techonology Incorporation and a microSD flash memory card, which allows data to be write and read onto it when inserted into a card shield reader. The microSD flash memory card is a non-volatile storage device. The card shield reader uses serial peripheral interface (SPI) protocol to communication with the microcontroller in order to allow storing of data into microSD card over a time. The data are saved in plain excel format in a file stored into a SD card. This file can be down-loaded to the computer and extracted for further analysis.

2.6. Power Supply

The complete assembled seismograph was powered with a voltage of 12 V obtained from lithium battery through voltage pin (V_{in}) of the Arduino microcontroller. Other components of the device such as ADC boards are powered with 3.3 V, the multiplexers and the microSD card shield are powered with 5 V voltage supply respectively. These voltages are obtained from the generic power output on the Arduino microcontroller board. The power supply was back up with solar panel to charge the battery when required.

2.7. Description of Operation of the Developed Seismograph

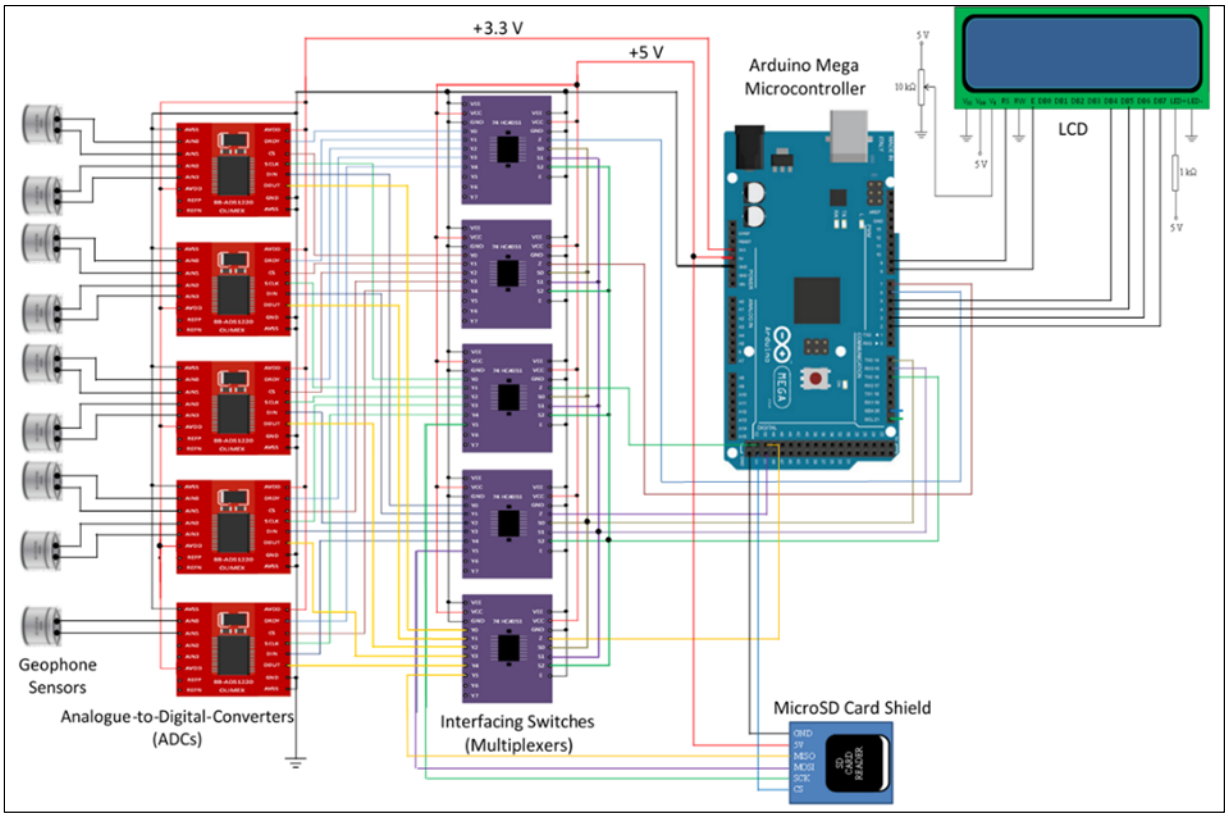

Figure 9 Complete Circuit Diagram of the Developed Seismograph

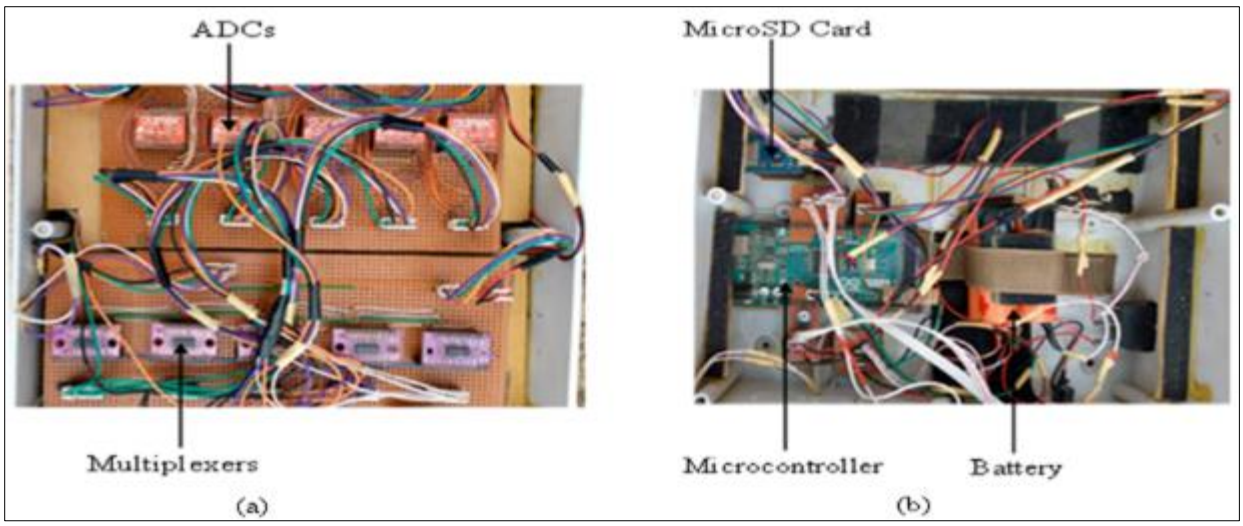

Figure 10 (a) Hardware Connection of Analogue-to-Digital Converters (ADCs) with Multiplexers (Digital Controlled Analogue Interfacing Switch) (b) Internal Circuitry of the Developed Seismograph

The operation of the seismograph begins with the response of the geophone sensors to seismic vibration signal. The geophones convert the ground motions (vibrations) detected into corresponding varying electrical voltage signals. Meanwhile, the signals are generally very weak and small in value in the order of few millivolts (mV). These signals are passed to the ADC modules through their differential input channels as indicated in the complete circuit diagram of the seismograph shown in Figure 9. Furthermore, each channel of the ADCs is integrated with built-in programmable gain amplifiers (PGAs) which help to amplify the geophones' signals to the Full-Scale Range (FSR) of the ADCs before being

digitized. The ADCs convert the amplified signals into sequence of serial digital values and these values are inputted onto the microcontroller through serial peripheral interface (SPI) communication protocol. Both the ADCs and the micro SD card reader share this bus to communicate with the microcontroller, thus, to prevent the ADCs' outputs and the micro SD card reader from being interfering with one another when communicating with the microcontroller, a digitally controlled analogue switch, using 8-to-1-line multiplexer board is employed to simultaneously select which of the ADCs is to be connected with microcontroller based on the instruction sets given to it by the microcontroller. The microcontroller processes the digital signals into readable values that are corresponding to the levels of ground vibrations detected. Further to this, these values are displayed on the LCD for physical visualization and also stored into the micro SD card for further analysis to determine the magnitude of the vibration levels that occur in given areas. Figure 9 shows the complete circuit diagram of the developed seismograph. Figures 10a and 10b shows the hardware connection of ADCs and multiplexers, and internal circuitry of the developed seismograph.

2.8. Testing and Calibration

Each unit of the developed seismograph shown above in Figure 9 was coupled together using flexible cables. The signal conditioning units of the developed seismograph, specifically the Analogue-to-Digital Converters (ADCs) were tested individually to ensure that they are working correctly and the data produced by them are reliable. In the testing procedure, a 1.5 V AA size battery type was used to provide input signals to the ADCs, a potentiometer was connected across the battery's terminals to adjust its voltage level to different values in order to provide input signals to the ADCs. The resulting outputs were monitored on the Arduino serial monitor window screen. In addition, a digital voltmeter was simultaneously used to monitor the voltage values across the potentiometer's wiper to check for the correctness of the values displayed on the Arduino serial monitor. Also, the multiplexer circuits, which serves an interface switch between the ADCs and microcontroller were tested and monitored using arrays of light emitting diodes (LEDs) indicators to ensure that they are switching correctly in the right sequence. The complete assembled seismograph was tested before being calibrated by exciting the geophones with footstep vibrations to ascertain its workability.

After this, the developed seismograph was calibrated against a standard seismograph by placing the two devices side by side to measure ground vibration due to a load mass of 10 kg dropped from 2 m high above ground. The data measured by the standard seismograph was used to check for the correctness of data measured by the developed seismograph. From this, some adjustments were made to the developed seismograph until the values displayed on it were approximately equal to the values displayed on the standard seismograph. After the necessary adjustments, the two devices were used to measure ground vibrations due to the falling weight device again and the results of the measurement are presented in Table 1.

The test was repeated several times under same conditions to ensure its accuracy, precision and reliability. The seismograph measures ground vibration levels in terms of peak particle velocity (PPV) (which is the vector sum of the three orthogonal ground vibration components detected by the instrument), using a threshold limit of 50 mm/s from International Standard Organization (ISO) and other related organizations to evaluate effects of ground vibrations due to quarry operations in given areas.

2.9. Experimental Setups and Field Tests

After the calibration process and verification of the workability of the developed seismograph, the seismograph was later deployed to two different site locations, including road carriageway at Ibese, Ogun State and road construction site at Oba-Ile, Ondo State, Nigeria respectively to measure ground motions due to vehicular movements and road construction works. The seismic sources were chosen with consideration of both technical and practical issues. Similarly, the site locations for the experimental setups and field tests were considered for several reasons such as proximity and ease of access for experimentation, and consequently low seismic ambient noise. Figures 11 and 12 present the experimental setups of the vibration measurements at these locations. At each site location, three measurement points were used, and each point was installed with triaxial geophone networks which were arranged along the same direction in a straight line at predetermined distances of 10 m, 20 m, and 30 m from the vibration sources. The data collected were analyzed in two different domains; time and frequency domains using Fast Fourier Transform (FFT) analysis with MATLAB tool in order to resolve in detail the frequency contents and amplitudes of the measured vibration signals obtained. The graphs of the results of the measurements are presented in Figures 14 and 15.

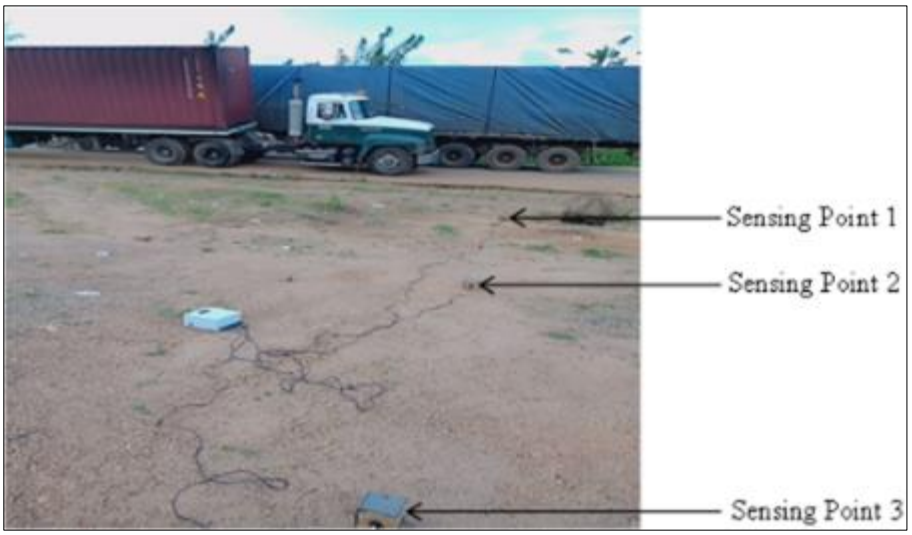

Figure 11 Experimental Setup along Road Carriage way at Ibese, Ogun State, Nigeria

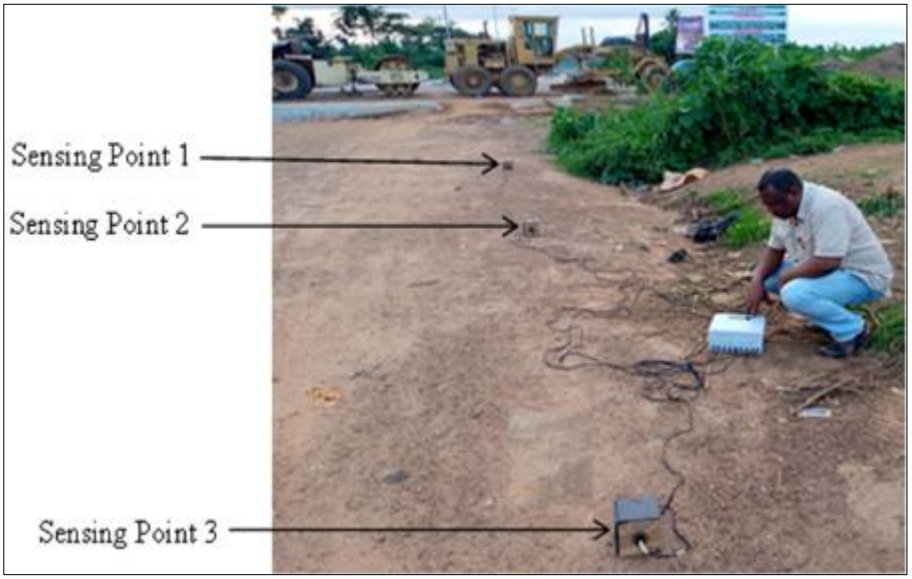

Figure 12 Experimental Setup at Road Construction Site in Oba-Ile, Akure, Ondo State, Nigeria

3. Results and Discussion

The performance evaluation of the developed seismograph was carried out by comparing the two sets of peak particle velocities (PPVs) presented in the Table 1. In the comparative study, a correlation analysis being a statistical method of examine the strength of relationship between two or more variables was performed. In the study, a plot of linear fit between the PPVs was carried out as shown in Figure 13. From the plot, a good strength of linear correlation (R^2 = 0.9987) which is very close to unity was obtained. This shows that the developed seismograph has a very good relation with the standard one; thus, this indicates that the developed seismograph is very reliable. From the analysis, it is showed that the developed seismograph exhibits slight deviation from the standard one with an accuracy of 99.87% and a tolerable error of ±0.13%, which is very insignificant. After calibration, the seismograph can measure ground vibration levels in terms of velocity between the range of 0.000017 mm/s to 143 mm/s with a sensitivity of 0.00000424 mm/s. The graphs shown in Figures 14 and 15 indicates the Fast Fourier Transform (FFT) analysis of the results of ground vibration levels measured along a road carriageway at Ibese, Ogun State and road construction site at Oba-Ile, Ondo State, Nigeria respectively. In order to give a better evaluation of the shape and frequency of the signals; data

recorded from all the three planes of the geophone networks at each measurement point were traced off separately; here, the X-axis is the frequency (Hz) and Y-axis is the vibration amplitude (mm/s).

According to the FFT analysis, the results show that for all three components of the geophones at each measurement point there is a significant difference between the vibration amplitudes. Also, the vibration amplitude levels obtained along the road carriageway at Ibese, Ogun State and road construction site at Oba-Ile, Ondo State were observed to be slightly higher than the vibration velocity threshold limit (> 50 mm/s) at certain distances from the source.

In addition, the vibration amplitudes were observed to be decreaseing with the increase of the distance between measurement points and the vibration sources. Figures 16 and 17 show the resulting attenuation curves of the vibration amplitudes obtained at the two site locations respectively. In this case, the obtained vibration amplitudes are studied as a function of distance. From the curves, it can be seen that the vibration amplitudes obtained at Ibese, Ogun State decays exponetially, which implies that the vibration strength diminish rapidly as they move away from source, thus, minimizing their potential impact on structures and human perception. Vibrations in this pattern, even at a relatively large magnitude higher than vibration threshold limit, may only affect areas in close proximity to the source. While, the vibration amplitudes obtained at Oba-Ile, Ondo State due to construction work decays linearly, which indicates that the vibrations reduces at a consistent rate over distance from the source, thus, vibrations of this type often maintain a relatively consistent strength over a larger distance compared to vibrations with exponential decay patterns, hence, this type of vibrations may have potential effects over wider areas which may cause damages to the nearby buildings and other structures during construction activities.

Table 1 Result of Vibration Levels Measured by the Developed Seismograph and the Standard Seismograph

Developed Seismograph				**Standard Seismograph**			
Velocity along X-axis (mm/s)	**Velocity along Y-axis (mm/s)**	**Velocity along Z-axis (mm/s)**	**Peak Particle Velocity, PPV (mm/s)**	**Velocity along X-axis (mm/s)**	**Velocity along Y-axis (mm/s)**	**Velocity along Z-axis (mm/s)**	**Peak Particle Velocity, PPV (mm/s)**
-0.004520	0.033855	0.043831	0.055567508	-0.004740	0.035381	0.045081	0.057502864
-0.002640	-0.085530	0.042920	0.095731274	-0.002860	-0.086350	0.044870	0.097354091
-0.037530	-0.083940	-0.068600	0.114718719	-0.039710	-0.084260	-0.069520	0.116231072
0.038923	-0.043850	-0.069750	0.091120168	0.039612	-0.045670	-0.071170	0.093381092
0.027894	-0.056860	-0.068790	0.093505074	0.029401	-0.057380	-0.070820	0.095772416
0.076298	0.034870	-0.067820	0.107874251	0.078121	0.035340	-0.069470	0.110353465
0.073941	0.025824	0.082742	0.113931510	0.075752	0.027252	0.083872	0.116256395
-0.037850	-0.004475	0.081745	0.090193643	-0.039140	-0.004676	0.083465	0.092304988
-0.042830	-0.002676	-0.032870	0.054055590	-0.044920	-0.002886	-0.033120	0.055884433
-0.057860	-0.078890	-0.031740	0.102853485	-0.059420	-0.080410	-0.032960	0.105275192
-0.098210	-0.068920	-0.068870	0.138341055	-0.099440	-0.069640	-0.070610	0.140441501
0.066953	-0.002174	-0.078520	0.103212504	0.068213	-0.002266	-0.080270	0.105363281
0.074577	-0.001758	-0.068470	0.101256903	0.076905	-0.001886	-0.069920	0.103955483
0.037957	-0.119862	-0.068950	0.143393638	0.038716	-0.124936	-0.069580	0.148152992
0.038979	-0.131879	-0.028980	0.140539224	0.040528	-0.133596	-0.030430	0.142885951
-0.039640	0.000359	-0.030750	0.050169921	-0.041370	0.000373	-0.031280	0.051865735

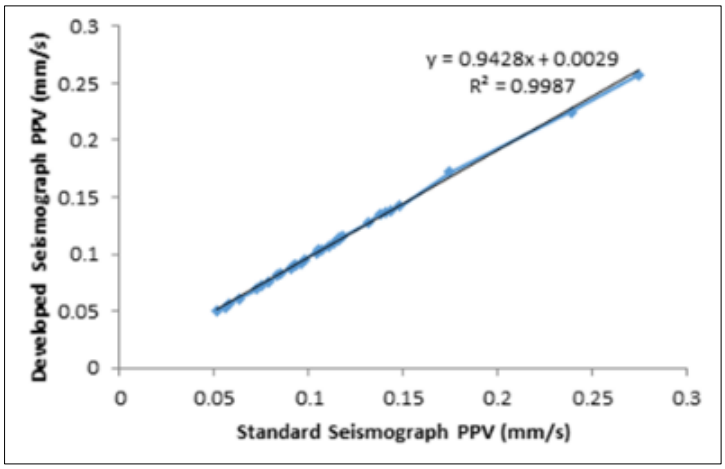

Figure 13 Trend of Peak Particle Velocity (PPV) Measured by the Developed and the Standard Seismographs

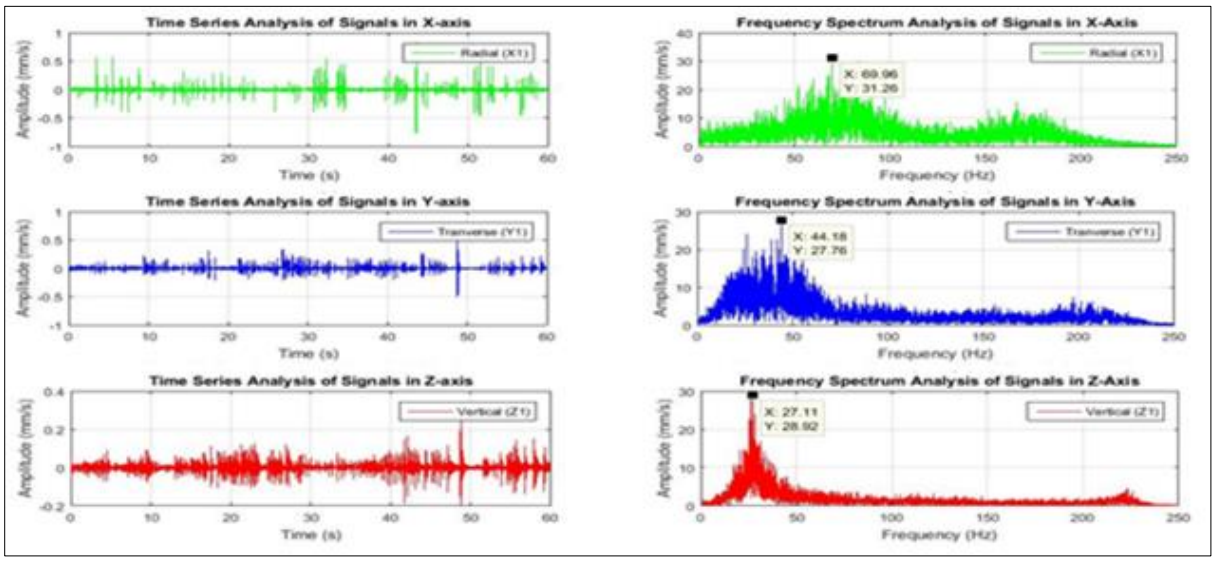

(a) Sensing Point 1 at 10 m away from the vibration Source

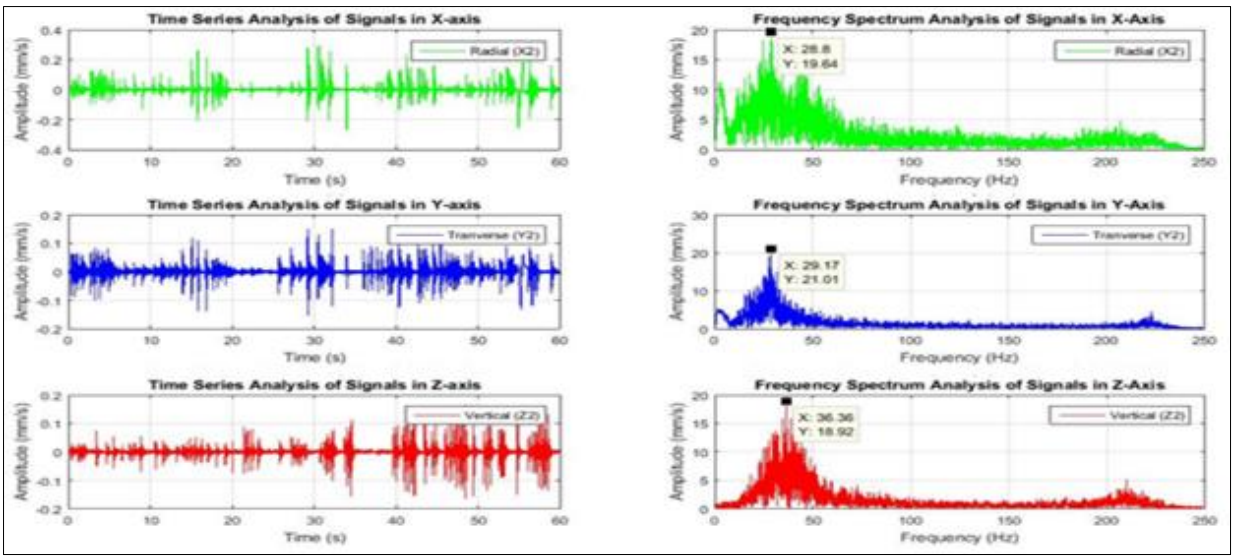

(b) Sensing Point 2 at 20 m away from the vibration Source

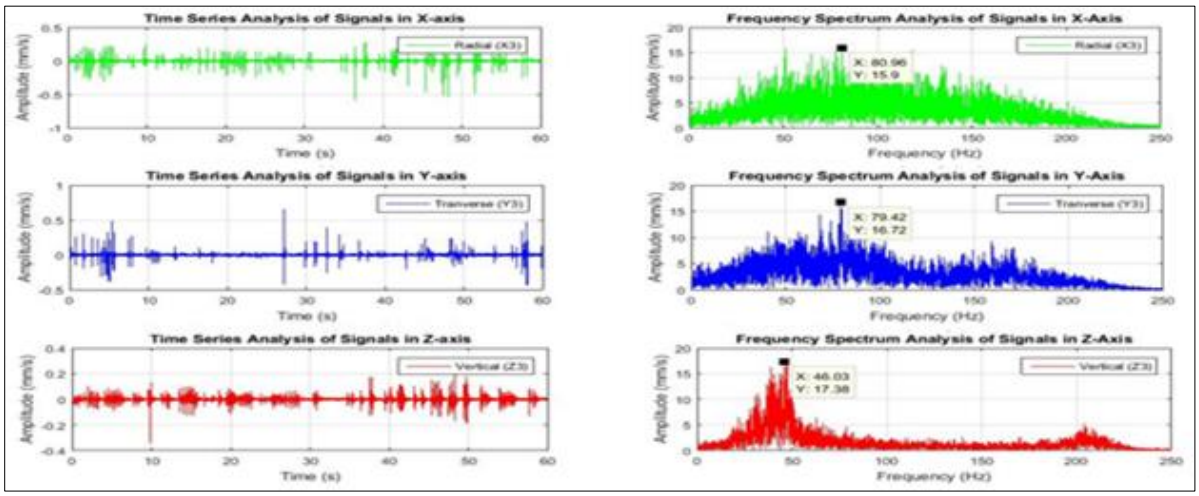

(c) Sensing Point 3 at 30 m away from the vibration Source

Figure 14 FFT Analysis of the Ground Vibrations Recorded at Ibese, Ogun State due to Vehicular Movements

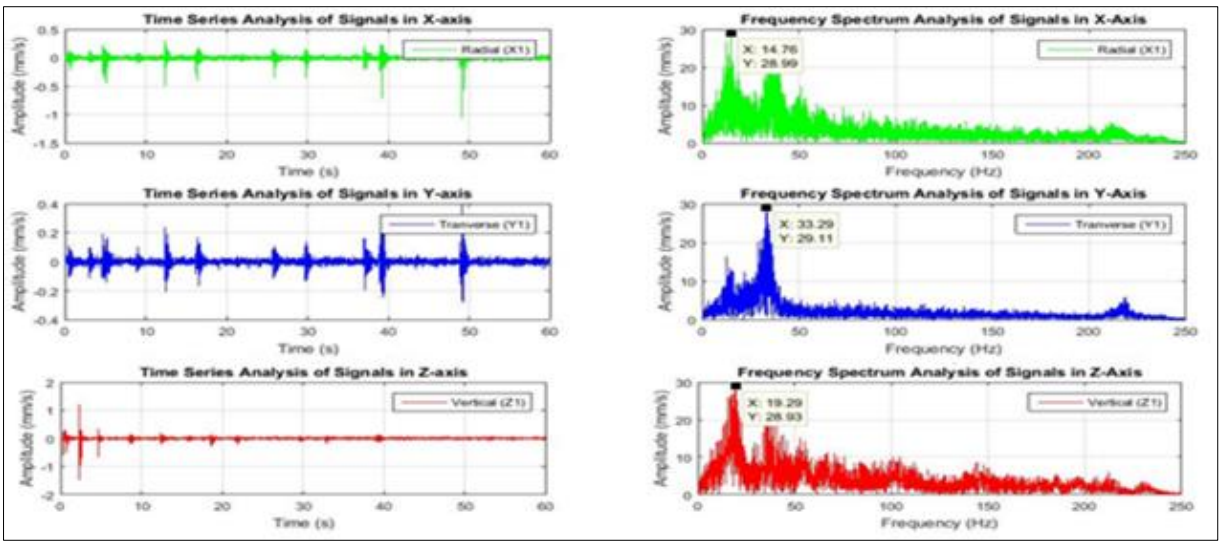

(a) Sensing Point 1 at 10 m away from the vibration Source

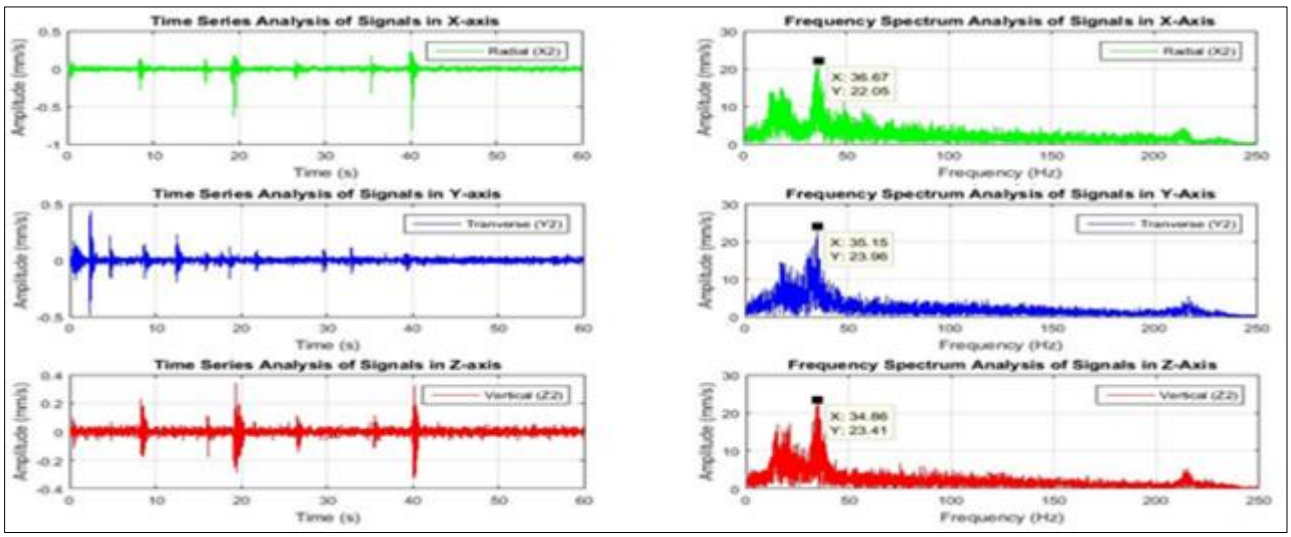

(b) Sensing Point 2 at 20 m away from the vibration Source

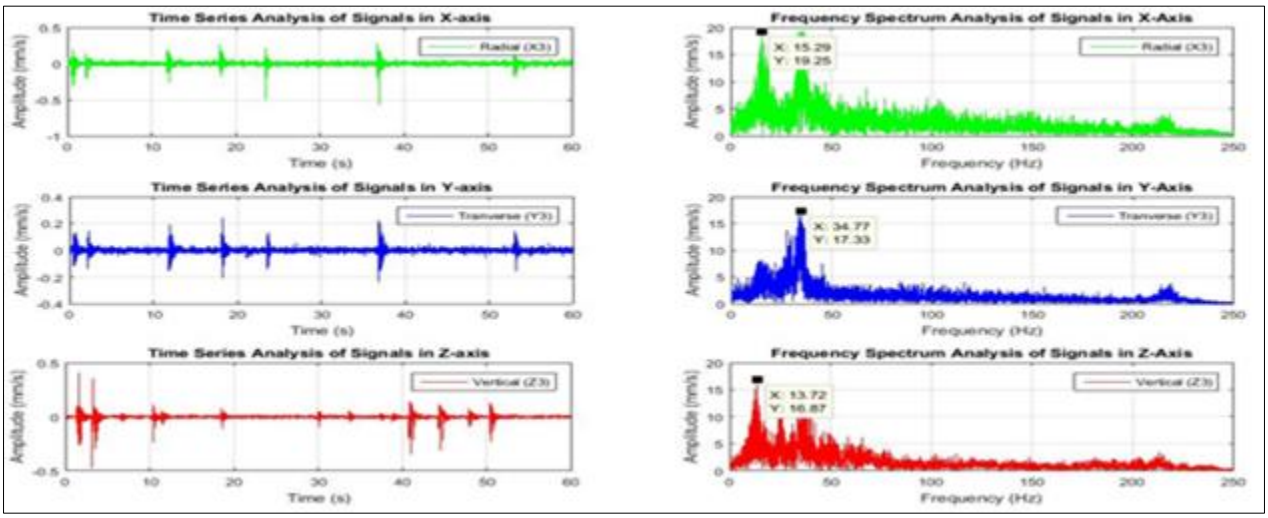

(c) Sensing Point 3 at 30 m away from the vibration Source

Figure 15 FFT Analysis of the Ground Vibrations at Oba-Ile, Ondo State due to Road Construction Work

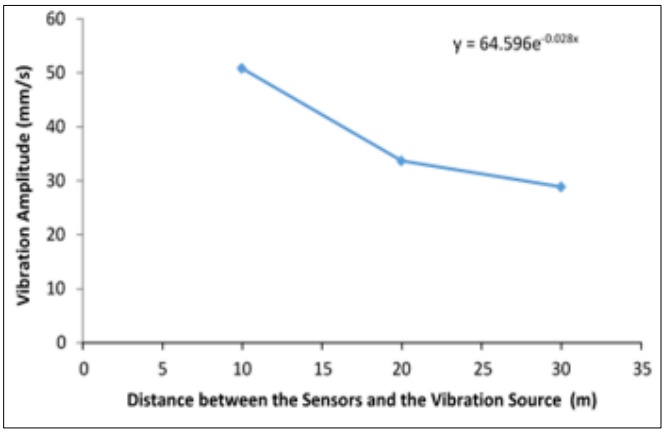

Figure 16 Attenuation Curve of Vibration Levels Recorded along Road Carriageway at Ibese, Ogun State, Nigeria

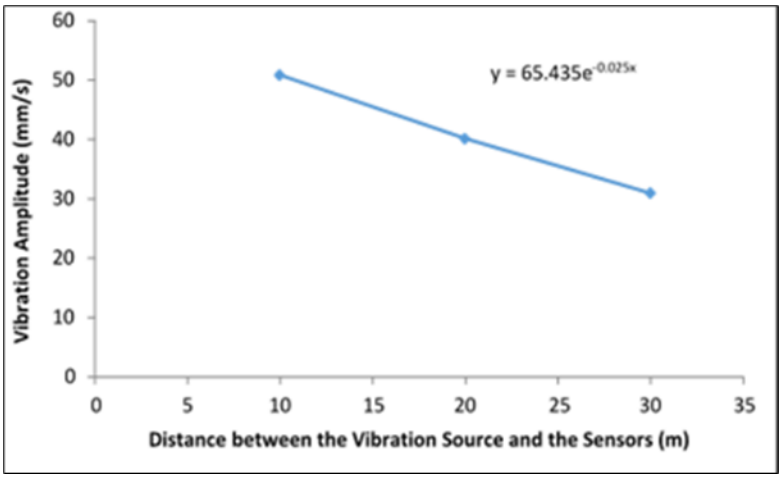

Figure 17 Attenuation Curve of Vibration Levels Recorded at Road Construction Site in Oba-Ile, Akure, Ondo State, Nigeria

4. Conclusion

This work unveiled the development of a 24-bit three dimensional (3D) seismograph for evaluation of seismic effects of earth disturbances due to seismic events mainly generated by human activities. The 3D seismograph, with its high accuracy and resolution, will provide valuable insight and comprehensive view of the seismic waves generated by both natural and human's activities and will be a valuable tool for decision-makers in the fields of seismology and civil engineering to understand how nearby structures behave during construction activities and this can help them to design better resistance measures that can withstand dynamic loads and prevent catastrophic failures. The 3D seismograph can also be used by government agencies to monitor the seismic activity in the region and provide early warning of potential seismic hazards. The technology represents an innovative way to measure and monitor the effects of earth disturbances caused by seismic events due to both natural and human's activities and provides a better understanding of the seismicity of the region.

Compliance with ethical standards

Disclosure of conflict of interest

No conflict of interest to be disclosed.

Statement of informed consent

- Conception, design and writing of the work: Adewumi Thompson Obagade
- Critical revision of the article: Sunday Emmanuel Falodun, Theophilus Ewetumo
- Final approval of the article to be submitted – all named authors approved the paper prior to submission: Adewumi Thompson, Sunday Emmanuel Falodun, Theophilus Ewetumo

References

[1] Alan, B. R., and Adrain, J. M. Blast Vibration Course: Measurement-Assessment-Control, Seventh Edition. Terrock Consulting Engineers, Terrock Pty Limited, Eltham Vic. 2005; 5-14.

[2] Alsadi, H. N. Seismic Hydrocarbon Exploration, Advances in Oil and Gas Exploration and Production. Springer International Publishing, Switzerland. 2017; 23–51.

[3] Haddad, Y. M. Mechanical Behaviour of Engineering Materials, Kluwer Academic Publishers. 2000; 82–83.

[4] Gutowski, T. G., and Dym, C. L. Propagation of Ground Vibration: A Review. Journal of Sound and Vibration. 1976; 49(2), 179–190.

[5] Milutin, S. Ground Vibration Engineering: Geotechnical Geological and Earthquake Engineering, Vol. 12. Springer Dordrecht Heidelberg, London. 2010; 1–29.

[6] Morbia, H. B., Sanghvi, C. S. C., and Bhavani, H. K. Impact of Road Traffic Vibration on Monument Structures. International Journal of Advanced Engineering Research and Studies (IJAERS). 2013; 2(3), 63-65.

[7] Norliana, S. Critical Review of Ground-Borne Vibration and Impact Assessment: Principle, Measurement and Modelling. Pertanika Journal of Scholarly Research Review. 2016; 2(1), 22–25.

[8] Anna, J., and Robert, J. Traffic-Induced Vibrations. The Impact on Buildings and People. The 9th International Conference ''ENVIRONMENTAL ENGINEERING", May 3-6 2014, Vilnius, Lithuania. 2014; 1–6.

[9] Andrea, E. D. G., and Paolo, B. Monitoring of Vibrations for the Protection of Architectural Heritage. 7th European Workshop on Structural Health Monitoring July 8-11, 2014. La Cité, Nantes, France. 2014; 639–640. https://hal.inria.fr/hal-01020409

[10] Ching-Jer, H., Hsiao-Yuen, Y., Chao-Yi, C., Chih-Hui, Y., and Chin-Lun, W. Ground Vibrations Produced by Rock Motions and Debris Flows. Journal of Geophysical Research. 2007; (Vol. 112), 1–12. https:// doi:10.1029/2005JF000437

[11] King, K. W., Algermissen, S. T., and McDermott, P. J. Seismic and Vibration Hazard Investigations of Chaco Culture National Historical Park: Open-File Report. 1985; 1, 1–43.

[12] Zdeněk, K., and Eva, H. Evaluation of Seismic Effect of Traffic-Induced Vibration. Acta Montanistica Slovaca. 2015; 20(1), 33–37

[13] David, T. Railway noise and vibration-mechanisms: Mechanisms, Modelling and Means of Control. Elsevier Limited, Oxford. 2009; 283–295.

[14] Aijun, C., Feng, C., Di, W., and Xianyuan, T. Ground Vibration Propagationt and Attenuation of Vibrating Compaction. Journal of Vibroengineering. 2019; 21(5), 1342–1352. https://doi.org/10.21595/jve.2019.20388

[15] Aliyu, D. S., Abdu, Y. A., and Yusuf, D. A. Transmission of Ground Vibration on Road Side Structures. European Journal of Advances in Engineering and Technology. 2016; 3(7), 43–46.

[16] Cenek, P. D., and Sutherland, A. J. Ground Vibration from Road Construction. Opus International Consultant Limited, Central Laboratories New Zealand Transport Agency Research Report. 2012; 1–48.

[17] Hunaidi, O., and Tremblay, M. Traffic-Induced Building Vibration in Montréal. Canadian Journal of Civil Engineering. 1997; 24(5), 736–753. https://doi.org/10.1139/197-023

[18] Henok, M. H. Measuring Traffic Induced Ground Vibration using Smartphone Sensors for a First Hand Structural Health Monitoring. Scientific African.2021; (11) 1–10.

[19] Mark, S., and Torben, R. L. Piezoelectric Accelerometers and Vibration Preamplifiers: Theory and Application Handbook. Bruel Kjaer, Denmark. 1987; 1–37.

[20] Adel, M. E. M., and Abuo, E. A. M. Quarry Blasts Assessment and their Envronmental Impacts on the nearby Oil Pipelines, Southeast of Helwan City, Egypt. National Research Institute of Astronomy and Geophysics (NRIAG) Journal of Astronomy and Geophysics. 2013; (Vol. 2), 102–104.

[21] Gang, W., Cai, W., and Shujin, L. Effect of Vibration from Highway Vehicle Load on Adjacent Buildings and its Assessment. IOP Conference Series: Earth and Environment Science. 2019; (article 267), 1–6. https://doi.org/10.1088/1755-1315/267/5/052048

[22] Ziaran, S., Musil, M., Cekan, M., and Chlebo, O. Analysis of Seismic Waves Generated by Blasting Operations and their Response on Buildings. World Academy of Science, Engineering and Technology: International Journal of Environmental and Ecological Engineering. 2013; 7(11), 769–774.

[23] Jordi, T., Mario, R., Pilar, S. S. P., and Paula, R. Urban Seismology: On the Origin of Earth Vibrations within a City. Scientific Reports, 2017; 1-6. https://doi.org/10.1038/s41598-017-15499-y

[24] Rui, X., Xunchang, L., Wei, Y., Minou, R., Chenglong, Y., and Songtao, X. Field Measurement and Research on Environmental Vibration due to Subway Systems: A Case Study in Eastern China. Multidisciplinary Digital Publishing Institute (MDPI). 2019; 1–11.

[25] Hamish, A. Development of a Low-Cost Strong Motion Seismograph [Ph.D. Thesis]. Department of Civil Engineering, University of Canterbury, Christchurch, New Zealand. 2005; 33–64.

[26] Picozzi, M., Milkereit, C., Parolai, S., Jaeckel, K., Veit, I., Fischer, J., and Zschau, J. GFZ Wireless Siesmic Array (GFZ-WISE), a Wireless Mesh Network of Siesmic Sensors: New Perspectives for Seismic Noise Array Investigations and Site Monitoring. Multidisciplinary Digital Publishing Institute (MDPI). 2010; 3281–3301.

[27] Claudia, A., Marcel, H., Bruno, F., Christoph, G., and Jose, M. Transformation of Ground Vibration Signal for Debris-Flow Monitoring and Detection in Alarm Systems. Multidisciplinary Digital Publishing Institute (MDPI). 2012; 4871–4888.

[28] Satish, S., Raghavan, R. V., Sarma, A., Suresh, G., Sateesh, A., Jitendar, P., and Srinagesh, D. A Study of Seismograph Setup in Schools to Educate and Awareness. International Organization of Scientific Research Journal of Research and Method in Education (IOSR-JRME). 2014; 4(5), 20–24. https://doi.org/10.9790/7388-04562024

[29] Deekshit, V. N., Maneesha, V. R., Indukala, P. K., and Nair, G. J. Smart Geophone Sensor Network for Effective Detection of Landslide Induced Geophone Signals. International Conference on Communication and Signal Processing, April 6-8, 2016, India. 2016; 1565–1569.

[30] Saraò, A., Clocchiatti, M., Barnaba, C., and Zuliani, D. Using an Arduino Seismograph to Raise Awareness of Earthquake Hazard Through a Multidisciplinary Approach. Seismological Research Letters, The Seismological Society of America. 2019; 87(1), 186–192. https://doi.org/10.1785/0220150091

[31] Soler-Lloren, J. L., Galiana-Merino, J. J., Giner-Caturla, J., Jaruegui-Eslava, P., Rosa-Cintas, S., and Rosa-Herranz, J. Development and Programming of Geophonino: A Low Cost Arduino-Based Seismic Recorder for Vertical Geophones. Computer and Geoscience. 2016; 3–19, https://dx.doi.org/10.1016/j.cageo.2016.05.014